

A STUDY OF THE COLLAPSE MECHANISM OF RIGID FRAMES BY ANALYSIS OF THE
ELASTO-PLASTIC SEISMIC RESPONSE USING A FLEXURAL MODEL

by Takayuki Teramoto (I)
Mitsugu Asano (II)
Haruyuki Kitamura (III)
Presenting Author: Haruyuki Kitamura

SUMMARY

This paper presents a study of the general collapse mechanism of rigid frames made by changing the bearing capacity of members as a parameter and using standard 10-story rigid frame models.

Analysis of the seismic response in the flexural model (full stiffness matrix type) is carried out by introducing elasto-plastic characteristics of the structural members into analysis.

INTRODUCTION

Presently, the so-called equivalent shear model (tri-diagonal stiffness matrix type) is usually used as the structural model in elasto-plastic response analysis. In the responses obtained from this model, however, unpredictable behaviour is sometimes observed. For example, the story slippage phenomenon, in which story displacement takes place only in certain stories in spite of the fact that most stories in this structure are sound, is seen in some cases. The authors were interested to determine whether this phenomenon would occur in actual practice. In order to study this subject, the seismic response was analyzed using a flexural model (full stiffness matrix type) obtained by introducing elasto-plastic characteristics of the structural members into analysis. As a result of a series of studies made by the authors on some actual buildings which were designed by them, it was clarified that the flexural model gives a smoother response distribution along stories than the equivalent-shear model¹⁾. The story slippage phenomenon which is observed in the equivalent shear model did not occur.

In this paper, a study is made of the collapse mechanism of a general rigid frame using a standard 10-story rigid frame model by changing the bearing capacity of members as a parameters. Items of study are shown in the following.

A comparative study is made of the response values of the flexural model and the equivalent-shear model.

For the flexural model, girder yield type and column yield type models were prepared. With the girder yield type, a study was made of the ratio between the girder yield moment and the column yield moment required for stable response behavior. Using the column yield type model, a study was made of the story slippage phenomenon.

Models in which the height-wise distribution of yield strength of structural members changes continuously and those in which the distribution changes in steps were prepared. Those models with continuous distribution have an ideal yield moment and stiffness distribution for response analysis. Step distribution models have distributions which are closer to those of actual buildings.

A structural model was prepared in which girder yield type frames and column yield type frames are combined together. By analyzing this model, a study was made of the ratio between the two yield type frames needed for stable response behavior.

MODEL FOR ANALYSIS OF SEISMIC RESPONSE

Steel Structure 10-story Rigid Frame Model

As shown in Fig. 1, a half-span frame was cut out from a multi-span rigid frame. By setting the boundary conditions of a pin roller on this frame, a continuous uniform rigid model was prepared. Story height (h), span (L) and weight per unit floor area were set to respective values of 3.8M, 6.4M and 0.6t/m².

Analysis for Assumed Member

With the weight of each story as a constant, a design story shear force Q_i was calculated using the latest aseismic design methods for buildings. At this time, the standard shear coefficient was taken as $C_0 = 0.2$.

$$Q_i = C_0 A_i \sum W_i$$

$$A_i = 1 + \left(\frac{1}{\sqrt{\alpha_i}} - \alpha_i \right) \times \frac{2T}{1+3T}$$

$$\alpha_i = \sum_{j=i}^N W_j / W_{\text{total}}$$

where, W_j : Weight of L story (t) $W_j = \text{const.}$
 W_{total} : Total wt. of building (t)
 T : First natural period (sec)
 H : Building height (m) $H = 38.0$ m
 N : No. of stories of building $N = 10$

On the assumption that the column and the girder have the same flexural rigidity, the stiffnesses of the column and the girder were set so that the ratio of the story displacement to the story height at the time of application of the design force was 1/200.

The design column moment was calculated on the assumption that the point of inflection on the column comes at mid height of the story. Similarly, the girder-end moment was taken as the mean value of the top moment of the lower column and bottom moment of the upper column. The yield moment of the column or the girder was taken as 1.25 times the design stress. However, the moment of the column bottom on the first story was taken as 1.5 times that of the column top, since the column bottom is considered restrained move.

Table 1 shows the constants in the analysis models. In practice this means that the members below can be fixed as follows:

Intermediate floor:	Girder	WH-700x200x12x19
	Column	□-500x500x16
Low floor:	Column	WH-700x250x12x22
	Column	□-500x500x19

Parameters for study

To study those items mentioned in the introduction, the 13 analysis models were used as shown in Table 2. For the shear model the equivalent shear spring is determined from the story displacement and the story shear forces for the design load of the flexural model. The yield story shear force was taken as 1.25 times the design story shear force. The distribution of the yield story shear force is shown in Fig. 2.

The ratio of the column yield moment to the girder yield moment (α) for the girder yield type models (CASE-1, 2, 1A and 2A) was taken as 2 values; namely, a column yield moment of 1.2 times and 1.5 times the girder yield moment. And, in the column yield type models (CASE-3 and 3A), the column yield moment was set to a value 0.83 times the girder yield moment.

For the height-wise distribution of stiffness and yield moment, 2 models were taken; namely, models (CASE-0, 1, 2 and 3) which change continuously and models (CASE-A, 1A, 2A and 3A) whose yield strength changes every 3 stories.

Fig. 3 shows the yield moment distribution of members used in the flexural model.

Models (CASE-5A, 5B, 5C, 5D and 5E) were taken by combining the girder yield type frame (CASE-2A) with the column yield type frame (CASE-3A) at ratios of from 1:9 to 7:3. Further, the secondary gradients of the equivalent shear spring and the member stiffness after the yield point were 0.01 times those within the elastic range.

STATIC ANALYSIS

Fig. 4 shows the ultimate stress diagram for gradually increased static load on the continuous models (CASE-1, 2 and 3) according to the lateral force distribution, which is the same as the design story shear force distribution. It is clear from this diagram that in the girder yield type models (CASE-1 and 2), the final state occurs after all the girder ends yield and the bottom of the lower story column also yields. And, in the columns yield type model (CASE-3), the final state occurs when the column top and the column bottom in a certain story yield at the same time.

NATURAL PERIOD AND NATURAL MODES

The natural period and natural modes of the shear models and the flexural models are shown in Fig. 5. Further, in order to eliminate different responses to the input wave due to changes in the natural period and the natural modes, the stiffness is continuously changed even in the step distribution model. The periods and modes are the same in all the models.

INPUT WAVE

With phase characteristics incorporating North-South components as in the seismic wave observed on the first floor of the Tohoku University building during the MIYAGI KENOKI earthquake of June 12, 1982, an input waveform was prepared with an acceleration spectrum agreeing with the R_t curve ($T_c = 0.6$ seconds) in the Japanese new aseismic design code for buildings. The magnitude of the input wave was equivalent to a standard shear coefficient of $C_0 = 1.0$ (maximum acceleration: 434 cm/sec^2).

$$SA/G = R_t C_0$$

$$R_t = \begin{cases} 1 & T \leq T_c \\ 1 - 0.2 \left(\frac{T_c}{T} - 1 \right)^2 & T_c < T \leq 2T_c \\ \frac{1.6T_c}{T} & 2T_c < T \end{cases}$$

T_c : The predominant ground period (Soil Profile Type 2: $T_c = 0.6 \text{ sec}$)

T : Natural Period of the Building ($T = 0.03H = 1.14 \text{ sec}$)

The input waveform and the response spectrum are shown in Figures 6 and 7.

PLASTIC HINGING AND DUCTILITY FACTOR

Fig. 8 shows the results of the seismic response analysis including the location of "plastic hinging", the maximum ductility factors (μ_m) of all the

members and the maximum ductility factors (μ_{max}) of all the stories. On the basis of the tangential angles formed by ends of the members when both ends reached their yield moments calculated on the assumption that the members undergo inverse symmetrical deformation, the ratio of the maximum tangential angle of response to the above tangential angle was set to μ_m .

The ratio of the maximum story displacement of the response to the yield story displacement of the shear model was set to μ_{max} .

A study of the step distribution models (CASE-1A, 2A and 3A) showed that no hinging occurs to the column in CASE-2A ($\alpha = 1.5$) of the girder yield type models. In CASE-1A ($\alpha = 1.2$), while hinging occurs on part of the columns, the ductility factor is small with a maximum value of approximately $\mu_m = 1.8$ at the most. In the column yield type model (CASE-3A), hinging occurs on all the columns, and while the ductility factor is large particularly in the 4th and 7th stories where the yield strength decreases (maximum: $\mu_m = 7.4$), it is small in the immediately above and below stories of the above. With respect to the continuous yield moment distribution models (CASE-1, 2 and 3), the location of hinging of the member is the same as for the step distribution models. The ductility factors of all the members, however, are smoothly distributed in height-wise.

MAXIMUM RESPONSE

A study on the maximum response was made by using data on the maximum story displacement (δ_{max}), the maximum story ductility factor (μ_{max}), and the nondimensioned energy (μ_e). The nondimensioned energy (μ_e), as seen in Fig. 9, results from dividing the story hysteresis energy (W_h) by the elastic limit strain energy (W_e : values from the shear models are employed).

Figures 10, 11, and 12 show the distributions for the maximum story, the maximum ductility factor and the nondimensioned energy, respectively. Shown in the graphs, in order from top to bottom, are the responses of the continuous yield strength distribution models (CASE-0, 1, 2 and 3), the step yield strength distribution models (Case-A, 1A, 2A and 3A) and the models (CASE-5A, 5B, 5C, 5D, 5E) combining the girder yield type frame (CASE-2A) and the column yield type frame (CASE-3A).

These figures show that the responses of the flexural models and the shear models were stable when the yield strength changed continuously.

When the yield strength changed on a step basis, the story slippage phenomenon occurred on the shear model and the column yield type model, and the response became extremely unstable. The responses of these two were very similar to each other. The girder yield type models show stable responses. The responses of the combined models became similar to the column yield type models as the ratio of the girder yield type frame decreased, and they also became more and more unstable.

On the other hand, the nondimensioned showed a remarkable plasticity when compared with the maximum ductility factor, and on the story where the plasticization was more advanced, it showed a 2 or 3 times as large as the maximum ductility factor.

INFLUENCE OF COMBINING FRAMES

Fig. 13 shows the trends of the 2nd, 4th and 7th stories, where the yield moment of the members varies, with the ratio of the girder yield type frame as the abscissa and the ratio of the story displacement of a certain story to the mean of the upper and lower story displacements (that is, the story slippage ratio) as the ordinate. This figure shows clearly that when the ratio of the girder yield type frame drops below 30%, the story slippage ratio becomes

extremely large indicating that the story slippage phenomenon has started. Fig. 14 shows the ratio of each story's hysteresis energy to the overall hysteresis energy. It is clear from this figure that when the ratio of the girder yield type frame drops below 30%, energy consumed as hysteresis energy concentrates on a particular story causing the story slippage phenomenon to progress further.

CONCLUSION

While the study was made on a limited number of cases, the results may be summarized as follows:

The response values for the shear model proved to agree fairly well with those of the column yield type flexural models.

In the frame models in which the yield strength changed continuously, both the flexural models and the shear models gave smooth response distributions in the height-wise direction. In the frame models in which the yield strength changed on a step basis, while the girder yield type models show response distributions in the height-wise direction, the story slippage phenomenon is seen in the shear models and the column yield type models.

The nondimensioned energy, which was calculated from the hysteresis energy, show a remarkable degree of plasticization compared with the maximum ductility factor.

In the girder yield type models, when the girder yield moment was 1.2 times as large as the column yield moment or more the response behavior was stable, although hinging occurred on some columns.

In the structural models combining the girder yield type frames and the column yield type frames, as long as the girder yield type frame occupied about 30% or more in a model, it showed a stable response behavior.

References

- 1) ELASTO-PLASTIC DYNAMIC RESPONSE ANALYSIS OF FLEXURAL SHEAR MODEL' 7 WCEE
by M. Asano and T. Teramoto

(I) Chief, Structural Department, Nikken Sekkei Ltd., Japan

(II) Structural Engineer, Nikken Sekkei Ltd., Japan

(III) Structural Engineer, Nikken Sekkei Ltd., Japan

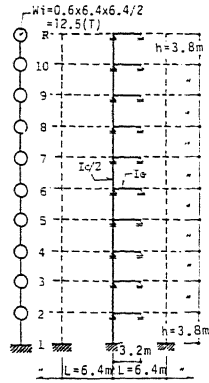


Fig. 1 Analysis Model

Distribution of Yield Moment	Analysis Model	Analysis Case	Yield Moment Ratio (0, 0)		C.Y.S. / G.Y.S.
			Girder	Column	
Continuous	Shear	CASE-0	1.25		
	Flexural	CASE-1	1.25	1.5	1.2
		CASE-2	1.25	1.875	1.5
		CASE-3	1.5	1.25	0.83
Step	Shear	CASE-A	1.25		
	Flexural	CASE-1A	1.25	1.5	1.2
		CASE-2A	1.25	1.875	1.5
		CASE-3A	1.5	1.25	0.83
Combining Frames		CASE-2A	CASE-3A		
Step	Flexural	CASE-5A	0.7	0.3	
		CASE-5D	0.5	0.5	
		CASE-5C	0.3	0.7	
		CASE-5D	0.2	0.8	
		CASE-5E	0.1	0.9	

Table 1 Constants of Analysis Models

	Weight Wi (t)	Ai	Shear Qi (t)	Ic/2 (cm ⁴)	Ic (cm ⁴)
R	12.5			10 ⁴	3.97
10	12.5	2.58	6.5	1.0%	6.31
9	12.5	2.05	10.3	3.16	8.25
8	12.5	1.79	13.4	4.13	9.91
7	12.5	1.61	16.1	4.96	11.33
6	12.5	1.47	18.4	5.67	12.53
5	12.5	1.36	20.3	6.27	13.51
4	12.5	1.26	22.0	6.76	14.35
3	12.5	1.16	23.3	7.18	14.96
2	12.5	1.06	24.3	7.48	15.39
1	12.5	1.00	25.0	7.70	

Table 2 Classification of Analysis Models

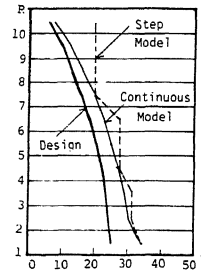


Fig. 2 Yield Shear Force Distribution of Shear Models

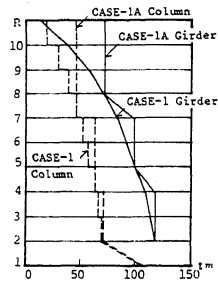


Fig. 3 Yield Moment Distribution in Member of Flexural Models

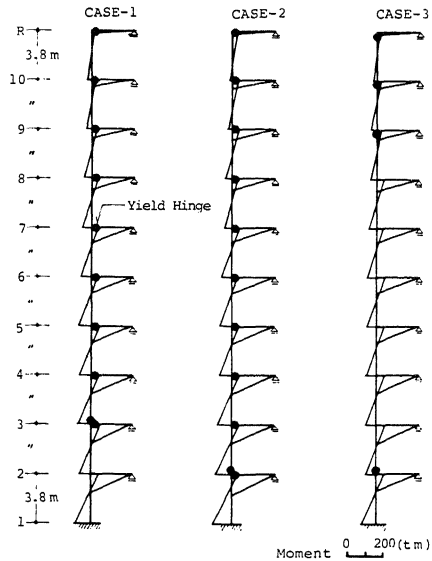


Fig. 4 Result of Static Analysis

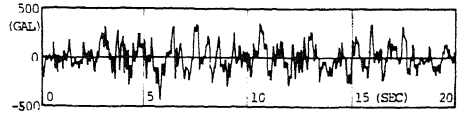


Fig. 6 Input Waveform

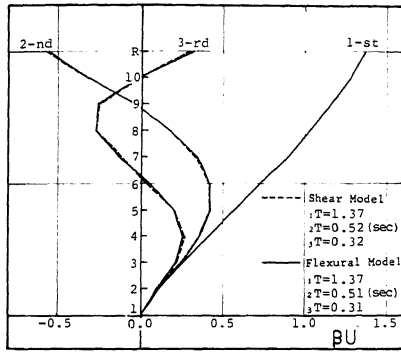


Fig. 5 Natural Periods and Natural Modes

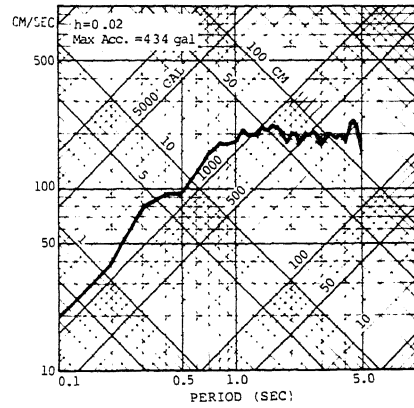


Fig. 7 Response Spectrum of Input Wave

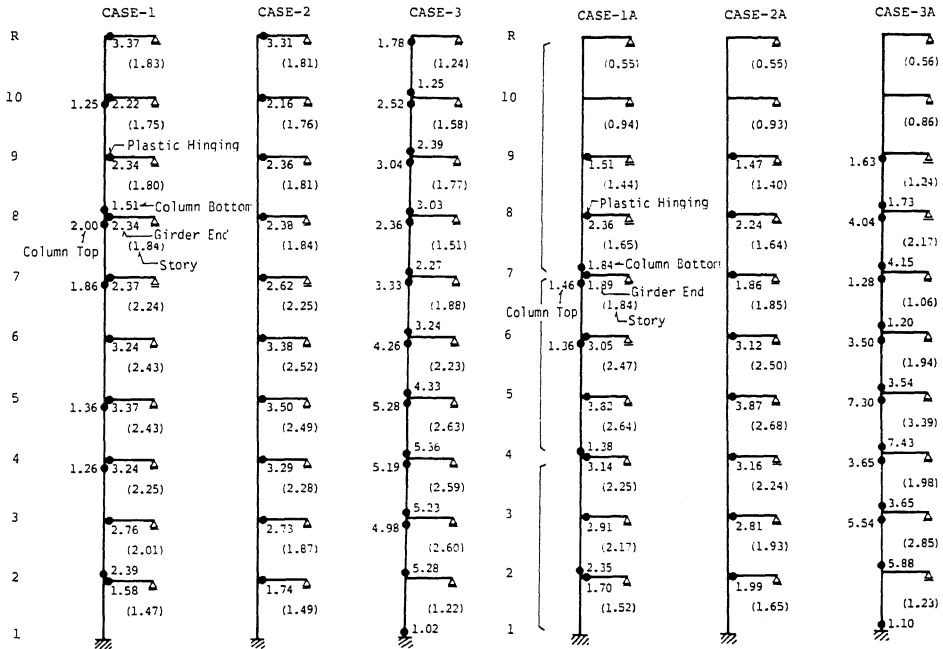
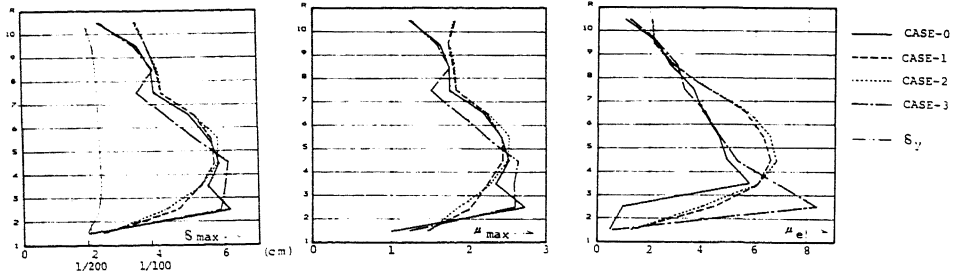
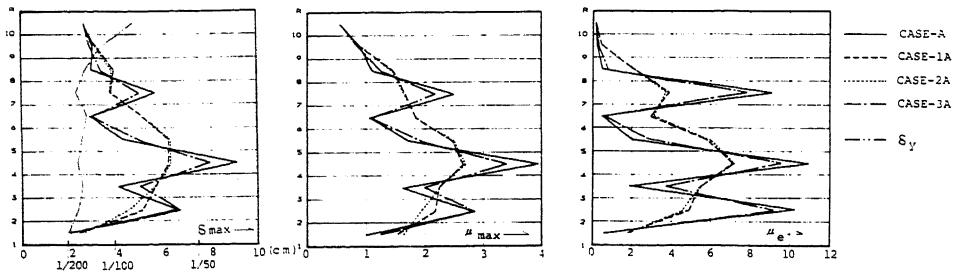


Fig. 8 Occurrence of Plastic Hinging and Ductility Factor

Continuous Distribution Models



Step Distribution Models



Combining Frames Models

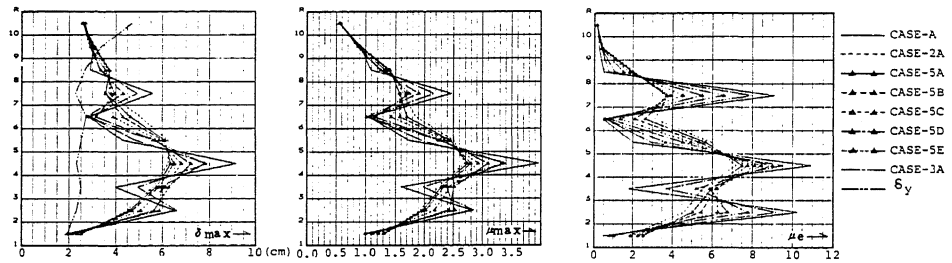


Fig. 10 Maximum Story Displacement

Fig. 11 Maximum Ductility Factor

Fig. 12 Nondimensional Energy

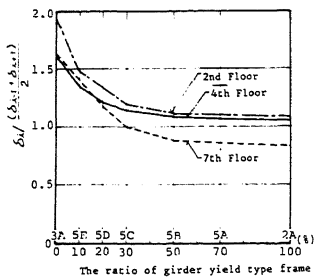


Fig. 13 Story Slippage Rate

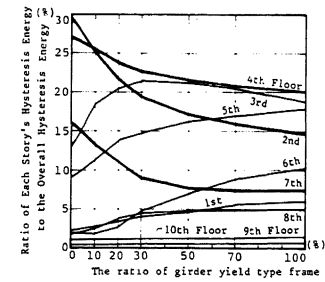


Fig. 14 Ratio of Each Story's Hysteresis Energy to the Overall Hysteresis Energy

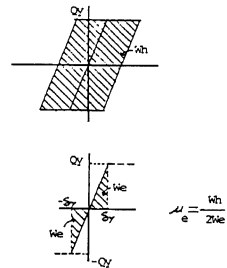


Fig. 9 Nondimensional Energy